# Development of a single crystal sample holder for interfacing ultrahigh vacuum and electrochemical experimentation

Jared P. Bruce, Khanh-Ly C. Nguyen, Fabian Scholten, Rosa M. Arán-Ais, Juan J. Navarro, Jens Hartmann, Markus Heyde, and Beatriz Roldan Cuenya

openaccess

View Online     Export Citation     CrossMark

## ARTICLES YOU MAY BE INTERESTED IN

# Development of a single crystal sample holder for interfacing ultrahigh vacuum and electrochemical experimentation

View Online    Export Citation    CrossMark

Jared P. Bruce, [iD] Khanh-Ly C. Nguyen, [iD] Fabian Scholten, [iD] Rosa M. Arán-Ais, [iD] Juan J. Navarro, [iD] Jens Hartmann, Markus Heyde,[a] [iD] and Beatriz Roldan Cuenya [iD]

**AFFILIATIONS**

Fritz Haber Institute of the Max Planck Society, Department of Interface Science, Faradayweg 4-6, Berlin 14195, Germany

[a] Author to whom correspondence should be addressed: heyde@fhi-berlin.mpg.de

**ABSTRACT**

Electrocatalyst surfaces prepared under ultrahigh vacuum (UHV) conditions can create model surfaces to better connect theoretical calculations with experimental studies. The development of a single crystal sample holder and inert electrochemical cells prepared with modularity and chemical stability in mind would allow for expensive single crystals to be reused indefinitely in both UHV and electrochemical settings. This sample holder shows reproducible surface preparations for single crystal samples and consistent electrochemical experiments without the introduction of impurities into the surface. The presented setup has been used as a critical piece for the characterization of Cu(111) surfaces under $CO_2$ electrochemical reduction reaction conditions as a test case.

## INTRODUCTION

Carbon dioxide ($CO_2$) emissions have accelerated anthropogenic climate change on a global scale. Current requirements for energy consumption are only met by high value products produced by the fossil fuel industry. However, there is a growing movement to generate these products from more carbon neutral sources. Collection and conversion of $CO_2$ back into high-value feedstocks would allow for mitigation of these effects on climate. In order to achieve this goal, electrocatalysts, such as copper (Cu), are being explored for their selectivity to $C_{2+}$ products in the carbon dioxide electrochemical reduction reaction ($CO_2RR$).[1–5] Other materials and reactions of interest include Pt for the oxygen reduction reaction (ORR) in fuel cells[6–9] or Earth-abundant metal phosphides for both the hydrogen evolution reaction (HER) and oxygen evolution reaction (OER) in water splitting.[10–12]

Heterogeneous reactions, such as those mentioned above, are dependent on both the chemistry and structure of the surface. In the past, model reactions were limited to gas/solid interactions and required ultrahigh vacuum (UHV) chambers for ultimate control

of the surface in order to fundamentally understand heterogeneous catalysis. However, with the prevalence of the liquid/solid interface, more work has been focused on understanding this interface with similar UHV instrumentation. This has presented its own set of challenges and has led to many developments in instrumentation that incorporates electrochemical cells into UHV chambers.[13–19] These developments have enabled simple electrochemical characterization, such as cyclic voltammetry, but are yet to incorporate online gas phase analysis critical for understanding electrocatalytic activity. An area that has received less attention is the development of sample holders that can preserve the sample preparation completed in the UHV chamber while being incorporated into standard electrochemical glassware, such as an H-type cell. There are many examples of commercial holders from a variety of vendors (Gamry Instruments, CH Instruments, and Redoxme AB) that are designed for corrosion experiments rather than for small single crystals (<10 mm diameter). Furthermore, careful control of the exposed area to the electrochemical solution is of critical importance when benchmarking the performance of different single crystal surfaces.[20] It should also be noted that the control of UHV sample preparation and characterization methods is often limited to the inner area of single crystal

surfaces due to certain beam focusing restrictions depending on the used methods.

In the electrochemical community, single crystal studies are conducted in a "hanging meniscus" configuration, often with noble metal samples, such as Pt, Pd, or Ir.[6] This method has been crucial for the understanding of the electrochemical behavior of single crystal surfaces. However, there has been limited characterization and development for *ex situ* single crystal preparation procedures where the surface structure and chemistry are comparable to UHV-prepared samples in metals other than those highlighted previously. Herein, we present a sample holder designed with UHV prepared single crystals in mind, enabling these samples to be transferred from UHV to the electrochemical cell and back to carry out post-mortem analysis on the catalyst surface with UHV instrumentation. This is a significant advantage to the hanging meniscus setup that offers little flexibility to be incorporated into a UHV setup to investigate the metal catalyst after the reaction. The presented sample holder is modular, simple, and created to allow for sample transfer from UHV to electrochemical cells and vice versa.

## EXPERIMENTAL

All UHV preparation and characterization were completed in one of two different chamber setups. Both setups had a base pressure of $<5 \times 10^{-10}$ mbar and were equipped with electron beam heating, argon sputtering, and low energy electron diffraction (LEED). All samples were prepared by alternating cycles of sputtering and annealing in vacuum.[21] Sputtering was carried out at 600 V and a sample current of 8–10 $\mu$A for 30 min followed by annealing in vacuum at 650 °C. LEED measurements (Omicron SpectaLEED, Scienta Omicron) were done with a filament current of 1.6 mA and a screen voltage of 6 kV. One chamber was equipped with an Auger electron spectrometer, while the other has a low temperature scanning tunneling microscope. STM experiments were performed in a custom-built system operating at low temperature (5 K).[22] The topographic STM images were taken in constant-current mode using a PtIr tip.

Auger electron spectroscopy was carried out with a spectrometer (DESA 150, Staib Instruments GmbH) equipped with a cylindrical mirror analyzer. All spectra were taken at an electron energy of 3 kV, a retarding ratio of 1%, and a step size of 1 eV from 40 to 1000 eV. Spectra were then analyzed by differentiating the raw data using a five-point Savitzky–Golay algorithm to generate the resulting spectrum using CasaXPS. No further charge correcting was required, and the samples were well grounded.

## Single crystal sample holder

In Fig. 1, a photograph for the sample holder in UHV and a schematic drawing for the electrochemistry sample holder are shown. The dimensions of the drawing are tailored to a sample that is circular and 10–7 mm in diameter. The opening for the sample exposure is 0.48 cm in diameter and gives a geometric electrochemical surface area of 0.181 cm$^2$ around the center of the sample.

UHV preparation of the surface is controlled near the center of the sample and becomes less defined near the edges, creating the need to define a consistent exposed area for the electrochemical experiments. All parts are shown in the breakdown of the holder in Fig. 1(b) with (8) representing the sample itself. All parts are fabricated with polyether ether ketone (PEEK), and sealing was achieved with Viton o-rings [FPM (fluorinated rubber polymer) Plate-Shore 70°, Reichelt Chemietechnik GmbH + Co.] of appropriate size and thickness for each setup. PEEK is easily machined with a material readily available rather than relying on specialized glassware. It is also chemically durable and inert toward a wide range of solvents, even those incompatible with glass. In some cases, especially for easily machinable metal single crystals, the ability to reduce the small space between the crystal surface and the holder exit will be
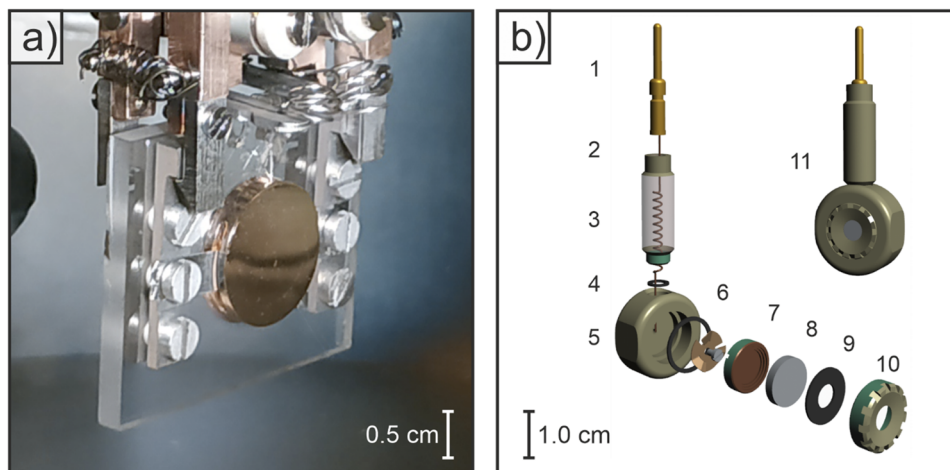


**FIG. 1.** (a) Cu(111) sample mounted on the holder in UHV conditions. The UHV sample holder was fabricated in-house and can be found elsewhere.[23,24] (b) Schematic drawing of a single crystal electrochemistry holder: (1) electrical pin, (2) copper wire, (3) outer polyether ether ketone (PEEK) pole connector, (4) Viton o-ring, (5) outer PEEK holder, (6) Viton ring and copper connector to the holder and screw, (7) sample seat, (8) sample, (9) Viton o-ring, and (10) outer PEEK threaded connection.
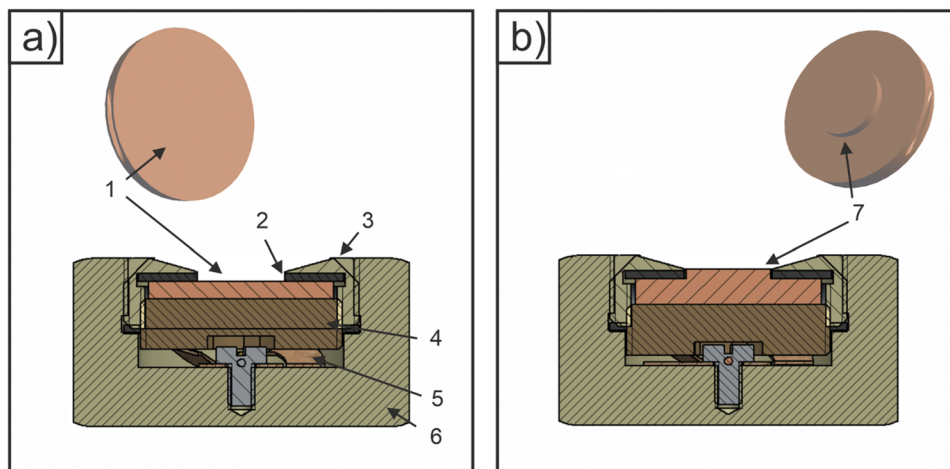
**FIG. 2.** Possible configuration for machinable metal single crystals. (a) Normal single crystal configuration: (1) surface of the single crystal, (2) Viton o-ring above the crystal face, (3) inner holder for the crystal, (4) inner o-ring, (5) back contact for the crystal, and (6) PEEK holder. (b) Machined single crystal configuration: (7) machined crystal incorporating the o-ring height.

important. To do this, one can cut a small area to match the holder as shown in Fig. 2.

The pole connection can be fabricated to any length desired. In our experiments, the length was tailored to an H-type electrochemical cell and could easily be used with electrochemical glassware or custom-fabricated PEEK H-type cells as shown in Fig. 3. A significant novelty of this holder is its ability to prevent damage to the single crystal surface and the fact that it allows the crystal to be used multiple times for different experiments. Single crystal surface preparation can be carried out in UHV conditions by mounting the sample on the holder as shown in Fig. 1(a), while the electrochemical work is done by removing the sample from the UHV holder and

mounting it in the electrochemical holder. Mounting is completed *ex situ*, in air prior to putting into the solution for characterization. These components are also capable of being introduced into a glovebox for air-sensitive work or to prevent exposure to the atmosphere.

The custom PEEK H-type cell in Fig. 3 was fabricated to work with solvents unsuitable for glass. Multiple blocks can be put in series with one another to create more elaborate electrochemical cells. The locking mechanism is similar to those found on commercial furniture to allow for ease and speed of assembly. A summary of all relevant volume dimensions is given in Table I.
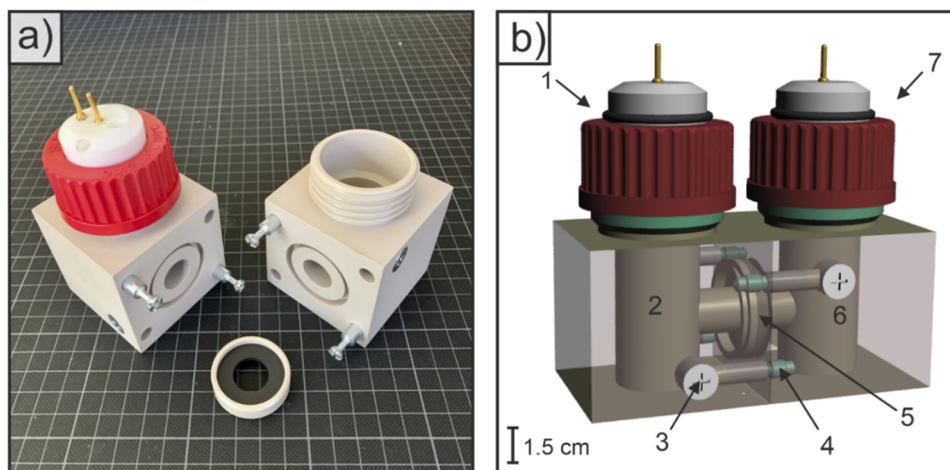


**FIG. 3.** Custom-fabricated PEEK H-type cell: (a) real image of the setup and (b) schematic representation of the PEEK cube cell: (1) cap with electrical feedthrough pins, (2) electrochemical cell compartment, (3) locking screw, (4) connector screw, (5) PEEK membrane holder with Viton seals, (6) locking screw, and (7) counter electrode compartment cap.

**TABLE I.** Summary of relevant dimensions for both the PEEK and glass H-type cells used in single crystal electrochemical experiments.

|  | Glass H-type cell | PEEK H-type cell |
|---|---|---|
| Total volume (ml) | 72.0 | 61.0 |
| Sample holder (ml) |  | 5.3 |
| Counter electrode (ml) |  | 1.5 |
| Cap (ml, ea.) |  | 18.0 |
| Electrolyte (ml) |  | 25.0 |
| Headspace (ml) | 23.7 | 12.7 |

### Electrochemical experiments

Two types of electrochemical experiments were carried out with these setups using a Gamry 1010E potentiostat (Gamry Instruments). The first is standard cyclic voltammetry carried out in 0.1M NaOH (Sigma Aldrich; trace metal basis) aqueous solutions. A scan rate of 50 mV/s was used for all voltammograms. These solutions were purged with Ar (Linde, 6N) for a minimum of 20 min prior to placing the samples in the solution. A 2 mm diameter, leakless Ag/AgCl reference electrode (eDaq) was used as the reference electrode, and a Pt mesh (Mateck) was used as a counter electrode. A PEEK electrochemical cell was used for the experiments in basic conditions as shown in Fig. 2 to avoid possible silicon contamination from a glass cell on the electrode surface in strongly basic conditions.[13] Samples were placed in the solution without applied potential and held at $-1.0$ V vs Ag/AgCl for 5 s prior to running the cyclic voltammetry experiments.

All carbon dioxide electrochemical reduction experiments were carried out in an H-type cell arrangement shown in Fig. 4 with further details given elsewhere.[25] $CO_2$ reduction electrolysis was carried out at $-1.1$ V vs the reversible hydrogen electrode (RHE) in $CO_2$ saturated 0.1M $KHCO_3$ for 1 h. The iR correction (current-interrupt mode) was applied during the electrolysis, and the conversion to the RHE scale was calculated by considering the pH of the solution. $CO_2$ was purged in both the cathodic and anodic compartments of the H-type cell at a flow rate of 20 SCCM for at least 30 min with two Bronkhorst mass flow controllers (Bronkhorst Deutschland Nord GmbH) regulated using in-house developed software built on the EPICS platform.[26–28] The external flow was checked with a flowmeter prior to attachment to the gas chromatograph to ensure no leaks in the system [Fig. 4(b)]. An Agilent gas chromatograph (GC, Agilent 7890B, model number: G3440B) equipped with a thermal conductivity detector (TCD) and a flame ionization detector (FID) and using $N_2$ as a carrier gas was used online to measure the gas phase products generated by the reaction. This GC was retrofitted with an automatic valve package and a nickel methanizer (Joint Analytical Systems) for controlling the gas injection into the columns. These experiments were often followed by off-line liquid product analysis with a high pressure liquid chromatograph (HPLC; Shimadzu Prominence) equipped with a NUCLOGEL SUGAR 810 column with a refractive index detector (RID) and a liquid phase gas chromatograph (L-GC; Shimadzu GC-2010 Plus) equipped with a Permabond CW20M column and a FID detector. Our experiments did not yield any liquid products during the reaction. A removable plexiglass housing is attached to the workstation around the electrochemical cell and can be attached to the building ventilation system to function as a small fume hood as shown in Fig. 5. The housing allows for hazardous gases, such as CO, to be used safely and effectively without a concern of leaking out into the laboratory environment.

Figure 5(b) also shows a combination setup for more advanced electrochemical characterization by a rotating disk electrode (RDE) experiment. The holder design was modified to fit in a standard rotator (Pine Research Instrumentation) and can be used for more advanced kinetic studies and diffusion experiments with UHV cleaned single crystal samples.
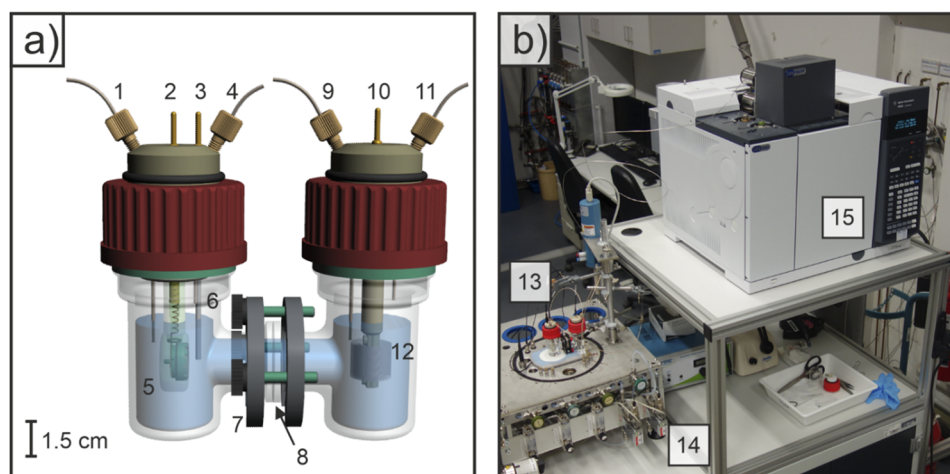


**FIG. 4.** (a) Schematic drawing of a custom-made H-type glass cell with a PEEK single crystal sample holder incorporated in the setup: (1) gas inlet, (2) electrical pin connection, (3) reference electrode pin, (4) gas chromatograph connection, (5) PEEK sample holder, (6) reference electrode, (7) screw tightened clamps, (8) Selemion membrane, (9) gas inlet, (10) counter electrode electrical pin connection, (11) gas outlet, and (12) counter electrode. (b) Real image of $CO_2$ reduction reaction with a glass cell and online gas chromatography: (13) integrated gas manifold electrochemical workstation, (14) Bronkhorst mass flow controllers for $CO_2$ flow, and (15) gas chromatograph.

**FIG. 5.** Electrochemical workstation with an integrated gas manifold for the delivery of desired gases. Possible configurations are visualized in (a) and (b): (1) Minican of the desired gas, (2) manual gas flowmeter, (3) automatic Bronkhorst gas flowmeter, (4) Plexiglass housing, (5) removable CF40 mount, (6) PEEK electrochemical cell, and (7) rotating disk electrode.

## RESULTS AND DISCUSSION

### UHV preparation of Cu(111) and post-mortem analysis

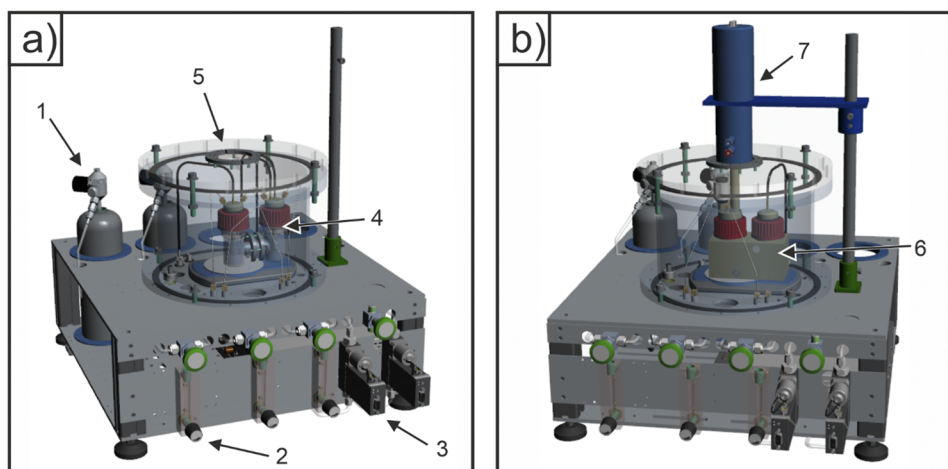Preparation of Cu(111) under UHV conditions is critical to understanding the effect of the surface structure and chemistry on the $CO_2$RR. Alternating cycles of sputtering and annealing were used to prepare the surface before a final anneal at 650 °C. Investigation of the surface was performed with STM prior to the removal of the sample from the vacuum [Figs. 6(a) and 6(b)]. STM characterization of the Cu(111) surface shows long terraces and step edges expected for Cu(111) with the closed-packed directions obtained from the atomically resolved image shown in Fig. 6(b). Both the LEED and Auger data indicate a clean Cu(111) surface [Figs. 6(c) and 6(d)]. There is no oxygen or carbon left after the cleaning, and the LEED pattern is sharp and consistent with the surface structure of Cu(111).[29]

Reintroduction of the sample into the UHV environment is crucial for any post-mortem analysis on an electrocatalytic system. The surface structure and chemistry could have changed during the reaction, and any adsorbates left on the surface will need to be thoroughly characterized. In Figs. 6(e) and 6(f), the LEED and Auger spectra of the same single crystal Cu(111) sample are shown. The Auger spectrum also shows new Auger peaks indicative of carbon and oxygen on the surface. Furthermore, there are no additional peaks from possible contaminants of Fe or Zn that have been reported in other studies, which may affect the $CO_2$ reduction at the surface.[30] These contaminants are normally observed by other methods in the literature, which shows that the crystal can be reintroduced into the UHV environment after electrochemical characterization.[30] The LEED characterization shows no diffraction spots at any energy, which is unsurprising given the exposure to the electrolyte solution; however, it is inconclusive regarding any structural changes of the surface that may be induced by the electrolysis. The

crystal can be regenerated by simple sputter/anneal cycles until the pristine surface is observed again [Figs. 6(c) and 6(d)].

### Electrochemistry

There are many advantages to designing and implementing an electrochemical holder for single-crystal electrocatalyst samples. The ability to prepare and characterize these samples in an UHV setting ensures that the surface of the catalyst will have a high level of reproducibility in terms of its structure and chemistry. One method that has been proposed as a benchmark for Cu catalysts is cyclic voltammetry characterization in basic conditions.[13,17] The advantage of this holder over a traditional hanging meniscus configuration is that there are no fixed connections to the crystal, the exposed surface area is well defined, and the sample is immersed completely within the solution, preventing any undefined edges and sides from being exposed. Herein, only the UHV prepared surface area of the single crystal is exposed to the electrolyte. A cyclic voltammetry experiment was carried out in 0.1M NaOH after sample removal from the UHV chamber and is shown in Fig. 7. A custom H-type cell was also fabricated out of the PEEK material (Fig. 2) and was used to carry out all cyclic voltammetry to avoid possible silica contamination on the Cu surface from the glass cell.[15]

The CV experiment shows similar results to other works in the literature for Cu(111) in basic solution.[31–34] Successive CVs were obtained by placing the holder in the cell without any applied potential or electrodes attached. Each successive scan was increased by 100 mV into the next larger, anodic potential window. The resulting CVs show a complex voltammetric response at high anodic potentials relative to the starting voltage. In the narrow scan window, two well-defined peaks exist, likely associated with the desorption of OH from the surface. This region is often used as a metric for assessing the surface adsorption of different Cu facets in solution.[31,32,35] Comparison with another UHV-prepared sample from the literature
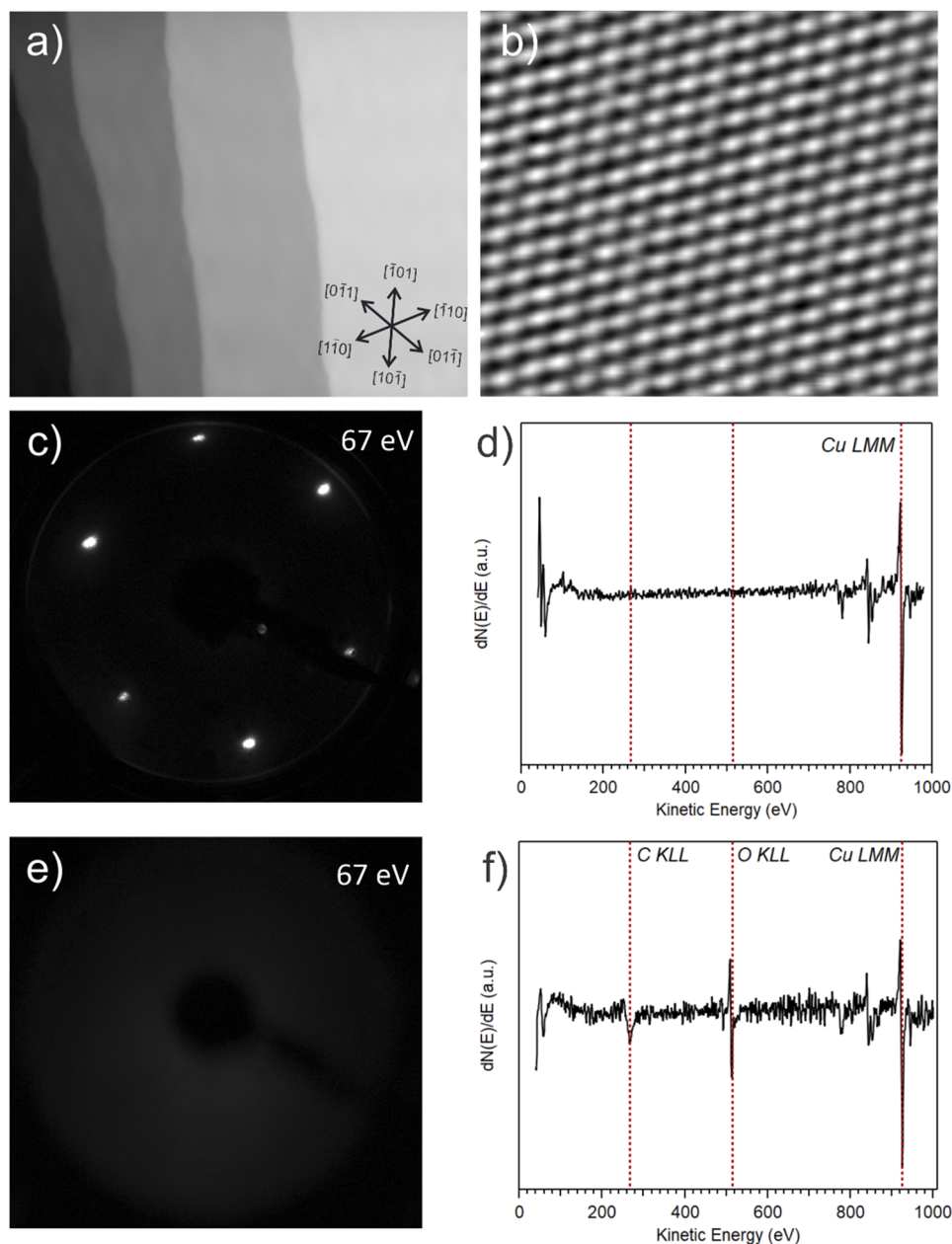
**FIG. 6.** STM images of the UHV prepared Cu(111) surface. (a) $100 \times 84$ nm$^2$, $V_s = 800$ mV, and $I_t = 50$ pA. Closed-packed directions of Cu(111) are represented by black arrows. (b) $3.5 \times 4.0$ nm$^2$, $V_s = 20$ mV, and $I_t = 2$ nA. The LEED images and corresponding Auger spectra of (c) and (d) freshly prepared Cu(111) and (e) and (f) Cu(111) after reintroduction into the UHV chamber after bulk electrolysis are shown.

(Fig. S1) shows a similar redox behavior with no indication of contamination.[31] The difference in current density is likely due to the uncertainty around the meniscus contact area relative to the well-defined area presented for this sample holder. The CV experiment shows that our electrochemical holder can provide a well-defined surface area, free of impurities, to investigate vacuum-prepared

single crystal samples. These electrochemical experiments were completed with the crystal transferred out of vacuum and mounted *ex situ* prior to being introduced into the solution. The reproduction of the electrochemical behavior in the CVs is encouraging, but if more stringent air-sensitive experiments are required, the holder and electrochemical setup are easily transferred to a glovebox for
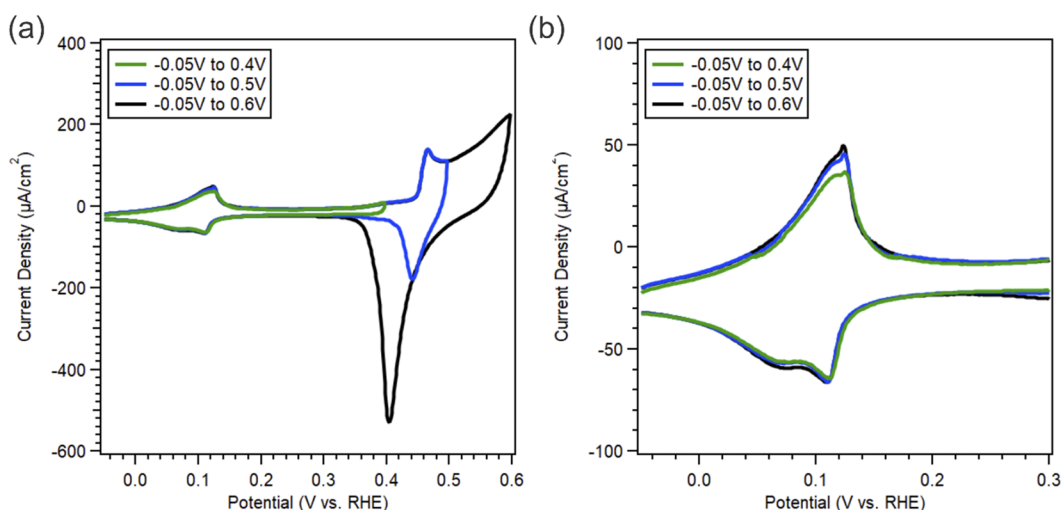
**FIG. 7.** Successive cyclic voltammograms of Cu(111) in 0.1M NaOH solution: (a) wide scan and (b) narrow scan. The scan rate for this experiment was 50 mV/s. The narrow scan highlights the region where OH desorption is expected to occur.

mounting and characterization. The UHV holder (with the sample still mounted) can also be transferred to a glovebox via a vacuum suitcase to be introduced to the glovebox under inert conditions.

Another area of interest for this holder is the use in electrocatalytic reactions. As alluded to previously, the holder was used for the electrocatalytic reduction of $CO_2$ on Cu(111) single crystal surfaces. The product distribution is an important metric often used to calculate the faradaic efficiency and selectivity of the reaction. A typical electrolysis is carried out at $-1.1$ V vs the reversible hydrogen electrode (RHE) after iR correction and generates a current density around $-4$ mA/cm$^2$. Table II shows a comparison of relevant $CO_2$ reduction product distributions from the literature.

The distribution of products for the Cu(111) surface at this potential is expected to have a significant amount of hydrogen produced with other carbon species produced as well. The distribution of products is intimately tied to the overpotential applied to the electrode. This leads to significant variations and presents a challenge for benchmarking any catalyst. The use of a well-defined surface and this type of electrochemical holder will help to standardize the variables associated with the catalyst efficiency. The observed spikes in the electrochemical data are expected to occur from bubble

formation near the surface of the electrode (Fig. S2). This is especially true for high amounts of hydrogen generated in flat surfaces. The product distribution is easily characterized by an online GC attached to the electrochemical cell while the electrolysis is running. A selection of relevant Cu(111) single crystal product distributions is shown in Table II. The electropolished sample presented here is very similar to that in the work by Huang *et al.*[3] and can also be compared with some of the original landmark work by Hori *et al.*[36] The electropolished Cu(111) preparations have a distinct product selectivity toward hydrocarbon products in addition to $H_2$. However, as we recently demonstrated,[37] the UHV prepared Cu(111) surface significantly favors the production of hydrogen. The high degree of control over the exposed area is key to obtaining this result and will be important moving forward when working with single crystals prepared using UHV instrumentation.

## CONCLUSIONS

The fabrication of the inert, modular sample holder has enabled the characterization of single crystal samples of interest to the electrocatalysis community under electrochemical conditions after

**TABLE II.** Comparison of $CO_2$ reduction reaction product distributions for different Cu(111) electropolished samples, including our UHV prepared Cu(111). Hori's data were completed under galvanostatic control at $-5$ mA/cm$^2$.[36]

| | Faradaic efficiencies (%) | | | | Partial current density (mA/cm$^2$) | | | |
|---|---|---|---|---|---|---|---|---|
| | H$_2$ | CO | CH$_4$ | C$_2$H$_4$ | H$_2$ | CO | CH$_4$ | C$_2$H$_4$ |
| Cu(111) epolish | 25 | 4 | 52 | 10 | 0.62 | 0.09 | 1.28 | 0.29 |
| Huang *et al.*[3] | 33 | 1 | 42 | 16 | 2.77 | 0.05 | 3.54 | 1.39 |
| Hori *et al.*[35] | 16 | 6 | 46 | 8 | ⋯ | ⋯ | ⋯ | ⋯ |
| Cu(111) UHV prep | 77 | 3 | 3 | 1 | 2.23 | 0.09 | 0.10 | 0.03 |

UHV preparation. The ability to prepare highly defined surfaces under UHV and then easily move those samples into an electrochemical environment without damaging the crystal is important to understanding the relationship between the surface structure and chemistry on the electrocatalytic reactions of interest. Furthermore, the well-defined area will be critical to benchmarking catalyst materials and surfaces moving forward. Contacts that are free of epoxy or adhesives allow these single crystal samples to be reused many times over. The plans and materials are very modular and will be important in further characterization of novel electrocatalytic materials important to energy research.

## SUPPLEMENTARY MATERIAL

See the supplementary material for additional electrochemical measurements and a comparison to data available from the literature.

## ACKNOWLEDGMENTS

## DATA AVAILABILITY

The data that support the findings of this study are available from the corresponding author upon reasonable request.

## REFERENCES

[1] K. J. P. Schouten, Y. Kwon, C. J. M. van der Ham, Z. Qin, and M. T. M. Koper, "A new mechanism for the selectivity to $C_1$ and $C_2$ species in the electrochemical reduction of carbon dioxide on copper electrodes," Chem. Sci. **2**(10), 1902–1909 (2011).

[2] A. A. Peterson and J. K. Nørskov, "Activity descriptors for $CO_2$ electroreduction to methane on transition-metal catalysts," J. Phys. Chem. Lett. **3**(2), 251–258 (2012).

[3] Y. Huang, A. D. Handoko, P. Hirunsit, and B. S. Yeo, "Electrochemical reduction of $CO_2$ using copper single-crystal surfaces: Effects of $CO^*$ coverage on the selective formation of ethylene," ACS Catal. **7**(3), 1749–1756 (2017).

[4] Y. Hori, A. Murata, R. Takahashi, and S. Suzuki, "Electroreduction of CO to $CH_4$ and $C_2H_4$ at a copper electrode in aqueous solutions at ambient temperature and pressure," J. Am. Chem. Soc. **109**(16), 5022–5023 (1987).

[5] R. M. Arán-Ais, D. Gao, and B. Roldan Cuenya, "Structure- and electrolyte-sensitivity in $CO_2$ electroreduction," Acc. Chem. Res. **51**(11), 2906–2917 (2018).

[6] R. Rizo, E. Herrero, and J. M. Feliu, "Oxygen reduction reaction on stepped platinum surfaces in alkaline media," Phys. Chem. Chem. Phys. **15**(37), 15416–15425 (2013).

[7] Y. Nie, L. Li, and Z. Wei, "Recent advancements in Pt and Pt-free catalysts for oxygen reduction reaction," Chem. Soc. Rev. **44**(8), 2168–2201 (2015).

[8] M. Shao, Q. Chang, J.-P. Dodelet, and R. Chenitz, "Recent advances in electrocatalysts for oxygen reduction reaction," Chem. Rev. **116**(6), 3594–3657 (2016).

[9] C. Zhang, X. Shen, Y. Pan, and Z. Peng, "A review of Pt-based electrocatalysts for oxygen reduction reaction," Front. Energy **11**(3), 268–285 (2017).

[10] X. Li and J. Wang, "Phosphorus-based electrocatalysts: Black phosphorus, metal phosphides, and phosphates," Adv. Mater. Interfaces **7**, 2000676 (2020).

[11] J. F. Callejas, C. G. Read, C. W. Roske, N. S. Lewis, and R. E. Schaak, "Synthesis, characterization, and properties of metal phosphide catalysts for the hydrogen-evolution reaction," Chem. Mater. **28**(17), 6017–6044 (2016).

[12] B. Kim, T. Kim, K. Lee, and J. Li, "Recent advances in transition metal phosphide electrocatalysts for water splitting under neutral pH conditions," ChemElectroChem **7**, 3578 (2020).

[13] D. K. Bora, P.-A. Glans, J. Pepper, Y.-S. Liu, C. Du, D. Wang, and J.-H. Guo, "An ultra-high vacuum electrochemical flow cell for in situ/operando soft X-ray spectroscopy study," Rev. Sci. Instrum. **85**(4), 043106 (2014).

[14] M. El-Jawad, J. L. Chemin, B. Gilles, and F. Maillard, "A portable transfer chamber for electrochemical measurements on electrodes prepared in ultra-high vacuum," Rev. Sci. Instrum. **84**(6), 064101 (2013).

[15] P. Kerger, D. Vogel, and M. Rohwerder, "Electrochemistry in ultra-high vacuum: The fully transferrable ultra-high vacuum compatible electrochemical cell," Rev. Sci. Instrum. **89**(11), 113102 (2018).

[16] M. P. Soriaga, "Ultra-high vacuum techniques in the study of single-crystal electrode surfaces," Prog. Surf. Sci. **39**(4), 325–443 (1992).

[17] M. P. Soriaga, J. H. Baricuatro, K. D. Cummins, Y.-G. Kim, F. H. Saadi, G. Sun, C. C. L. McCrory, J. R. McKone, J. M. Velazquez, I. M. Ferrer, A. I. Carim, A. Javier, B. Chmielowiec, D. C. Lacy, J. M. Gregoire, J. Sanabria-Chinchilla, X. Amashukeli, W. J. Royea, B. S. Brunschwig, J. C. Hemminger, N. S. Lewis, and J. L. Stickney, "Electrochemical surface science twenty years later: Expeditions into the electrocatalysis of reactions at the core of artificial photosynthesis," Surf. Sci. **631**, 285–294 (2015).

[18] J. Balajka, J. Pavelec, M. Komora, M. Schmid, and U. Diebold, "Apparatus for dosing liquid water in ultrahigh vacuum," Rev. Sci. Instrum. **89**(8), 083906 (2018).

[19] F. Reniers, "The development of a transfer mechanism between UHV and electrochemistry environments," J. Phys. D: Appl. Phys. **35**(21), R169–R188 (2002).

[20] K. Elouarzaki, V. Kannan, V. Jose, H. S. Sabharwal, and J.-M. Lee, "Recent trends, benchmarking, and challenges of electrochemical reduction of $CO_2$ by molecular catalysts," Adv. Energy Mater. **9**, 1900090 (2019).

[21] R. G. Musket, W. McLean, C. A. Colmenares, D. M. Makowiecki, and W. J. Siekhaus, "Preparation of atomically clean surfaces of selected elements: A review," Appl. Surf. Sci. **10**(2), 143–207 (1982).

[22] M. Heyde, M. Kulawik, H.-P. Rust, and H.-J. Freund, "Double quartz tuning fork sensor for low temperature atomic force and scanning tunneling microscopy," Rev. Sci. Instrum. **75**(7), 2446–2450 (2004).

[23] H.-P. Rust, T. König, G. H. Simon, M. Nowicki, V. Simic-Milosevic, G. Thielsch, M. Heyde, and H.-J. Freund, "A portable microevaporator for low temperature single atom studies by scanning tunneling and dynamic force microscopy," Rev. Sci. Instrum. **80**(11), 113705 (2009).

[24] S. Stuckenholz, C. Büchner, G. Thielsch, M. Heyde, and H.-J. Freund, "A portable quartz micro balance for physical vapor deposition techniques," Rev. Sci. Instrum. **84**(8), 085118 (2013).

[25] R. M. Arán-Ais, F. Scholten, S. Kunze, R. Rizo, and B. Roldan Cuenya, "The role of in situ generated morphological motifs and Cu(I) species in $C_{2+}$ product selectivity during $CO_2$ pulsed electroreduction," Nat. Energy **5**(4), 317–325 (2020).

[26] S. Dong, G. M. Huang, J. Frühauf, P.-A. Loizeau, I. Deppner, N. Herrmann, and D. Wang, "Detector control system for the CBM-TOF," J. Instrum. **15**(12), C12005 (2020).

[27] A. Das Gupta, A. K. Srivastava, S. Sunil, and Z. Khan, "Serial interface through stream protocol on EPICS platform for distributed control and monitoring," J. Phys. Conf. Ser. **823**, 012048 (2017).

[28] L. R. Dalesio, J. O. Hill, M. Kraimer, S. Lewis, D. Murray, S. Hunt, W. Watson, M. Clausen, and J. Dalesio, "The experimental physics and industrial control system architecture: Past, present, and future," Nucl. Instrum. Methods Phys. Res., Sect. A **352**(1–2), 179–184 (1994).

[29] J. J. Navarro, S. Tosoni, J. P. Bruce, L. Chaves, M. Heyde, G. Pacchioni, and B. R. Cuenya, "Structure of a silica thin film on oxidized Cu(111): Conservation of the honeycomb lattice and role of the interlayer," J. Phys. Chem. C **124**, 20942 (2020).

[30] A. Wuttig and Y. Surendranath, "Impurity ion complexation enhances carbon dioxide reduction catalysis," ACS Catal. **5**(7), 4479–4484 (2015).

[31] A. Tiwari, T. Maagaard, I. Chorkendorff, and S. Horch, "Effect of dissolved glassware on the structure-sensitive part of the Cu(111) voltammogram in KOH," ACS Energy Lett. **4**(7), 1645–1649 (2019).

[32] A. K. Engstfeld, T. Maagaard, S. Horch, I. Chorkendorff, and I. E. L. Stephens, "Polycrystalline and single-crystal Cu electrodes: Influence of experimental conditions on the electrochemical properties in alkaline media," Chem. - Eur. J. **24**(67), 17743–17755 (2018).

[33] S. Nitopi, E. Bertheussen, S. B. Scott, X. Liu, A. K. Engstfeld, S. Horch, B. Seger, I. E. L. Stephens, K. Chan, C. Hahn, J. K. Nørskov, T. F. Jaramillo, and I. Chorkendorff, "Progress and perspectives of electrochemical $CO_2$ reduction on copper in aqueous electrolyte," Chem. Rev. **119**(12), 7610–7672 (2019).

[34] A. Bagger, R. M. Arán-Ais, J. Halldin Stenlid, E. Campos dos Santos, L. Arnarson, K. Degn Jensen, M. Escudero-Escribano, B. Roldan Cuenya, and J. Rossmeisl, "*Ab initio* cyclic voltammetry on Cu(111), Cu(100) and Cu(110) in acidic, neutral and alkaline solutions," ChemPhysChem **20**, 3096–3105 (2019).

[35] A. Tiwari, H. H. Heenen, A. S. Bjørnlund, T. Maagaard, E. Cho, I. Chorkendorff, H. H. Kristoffersen, K. Chan, and S. Horch, "Fingerprint voltammograms of copper single crystals under alkaline conditions: A fundamental mechanistic analysis," J. Phys. Chem. Lett. **11**(4), 1450–1455 (2020).

[36] Y. Hori, I. Takahashi, O. Koga, and N. Hoshi, "Electrochemical reduction of carbon dioxide at various series of copper single crystal electrodes," J. Mol. Catal. A: Chem. **199**(1–2), 39–47 (2003).

[37] F. Scholten, K.-L. C. Nguyen, J. P. Bruce, M. Heyde, and B. Roldan Cuenya, "Identifying structure-selectivity correlations in the electrochemical reduction of $CO_2$: A comparison of well-ordered, atomically clean and chemically etched Cu single crystal surfaces," Angew. Chem. (to be published) (2021).